MEASUREMENT OF THE AXIAL DISPERSION COEFFICIENT OF COHESIVE POWDERS IN ROTARY KILNS

By

INGRID JOYLYN PAREDES

A thesis submitted to the

Graduate School-New Brunswick

Rutgers, The State University of New Jersey

In partial fulfillment of the requirements

For the degree of

Master of Science

Graduate Program in Chemical and Biochemical Engineering

Written under the direction of

Benjamin J. Glasser

And approved by

_____

_____

_____

New Brunswick, New Jersey

May 2016

ABSTRACT OF THE THESIS

Measurement of the Axial Dispersion Coefficient of Cohesive Powders in Rotary Kilns

By

INGRID JOYLYN PAREDES

Thesis Director: Benjamin J. Glasser

While continuous rotary calcination is a widely used thermal treatment in large-scale catalyst manufacturing, fundamental understanding of the process is absent from scientific literature. Thus, the goal of this research is to improve fundamental understanding of rotary calcination processes to aid in scale-up. For successful calcination to occur, the residence time of the particles must exceed the time required for heating and calcination. The optimal residence time therefore depends on both of these competing time scales, which are functions of feed material properties, kiln geometry and kiln operating conditions. For uniform treatment of the feed, the particles must also exhibit low axial dispersion. In this work, the residence time distribution and axial dispersion coefficient for two cohesive fluid cracking catalyst powders were measured in pilot plant kilns using a tracer study developed by Danckwerts. Results were successfully matched to the Taylor fit of the axial dispersion model and the Sullivan prediction

for mean residence time. It was found that an increase in feed rate, kiln incline and rotary speed decreased mean residence time and overall dispersion. The axial dispersion coefficient was found to vary with kiln conditions. Such results have not been previously reported for the cohesive powders such as the ones used in our work.

Acknowledgments

I would like to express the deepest appreciation for the members of the calcination project team. Kellie Anderson, Heather Emady, Bereket Yohannes, Bill Borghard, and my advisor, Professor Benjamin Glasser: thank you all for your mentorship. This work would not be possible without your patience, guidance and motivation. Maham Javed and Isaiah Chen, thank you for your assistance in the lab. It has been a pleasure to know and work with each of you and to have had the opportunity to collaborate with great scientists and engineers from the Catalyst Consortium outside of Rutgers as well. Al Maglio and Jean Beeckman, thank you in particular for hosting me as an intern and providing me with a valuable industry perspective on the work I have done while a student at Rutgers.

Dr. Helen Buettner and Dr. Fuat Celik, thank you for serving on my committee and for all you have done for me while an undergraduate at Rutgers. It has been a joy to be your student and to work with you as a member of Rutgers AIChE. I will definitely take the advice have given me over the past three years with me as I progress through my life and career.

To my siblings, Danielle and Dante Paredes, and to Richard Lu, Elliot Taylor, Joanne Horng, Jonathan Caverly, Marie Misterio, and Michael Pamula: thank you for always being there

for me and for all of the fun we have had at Rutgers. I could not ask for a more supportive group of friends.

Finally, to my mom and dad, Marlene and Dante Paredes, thank you for everything. This is for you.

Table of Contents

List of Tables

List of Illustrations

Chapter 1

Introduction

With applications in a wide range of solids manufacturing processes including blending, drying, and calcining, the rotary kiln has been established as an essential device in chemical and metallurgical industries [1]. The device's popularity stems from its apparently simple geometry – the kiln operates by allowing gravity and rotation to move granular material or powder from inlet to outlet. This mechanism has improved product quality in both batch and continuous processes [1], and researchers have performed analyses of the process since as early as the 1920's [2]. Still, the mass and heat transfer mechanisms governing the utility of rotary kilns remain a challenge to characterize and predict; developing fundamental understanding of rotary kiln processes will therefore greatly improve their scale-up from laboratory and pilot plant scales to the manufacturing scale.

In preparation of chemical catalysts in particular, a better scientific understanding of rotary kilns will improve continuous calcination processes in which the particle bed exchanges heat with a freeboard gas and the kiln wall as it rotates and moves axially along the kiln, as shown in Figure 1. Successful calcination occurs when the residence time exceeds the time required for calcination. The typically long residence times associated with rotary kilns favors uniform treatment of the feed [3], but long residence times lead to large material and energy costs. The key to successful and efficient calcination is therefore to minimize both the residence time and axial dispersion of particles within the kiln and to understand their relationship to the time required for calcination.

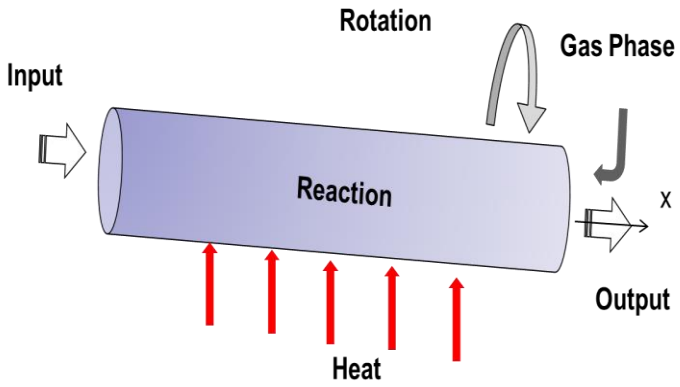

Figure 1. Schematic of Rotary Kiln

Radial and axial mixing are key factors that influence both residence time and calcination time, and modifications such as lifters and dams, in various sizes and shapes, have been installed in industrial kilns to improving mixing processes. Currently, no methodology exists correlating such modifications, kiln geometry and material properties with optimal operating conditions and residence times. It has been established, however, that the degree of particle mixing depends on the characteristics of the bed motion through the kiln. The mode of motion depends on rheological properties, fill level and rotation rate. Six modes of motion – centrifuging, cataracting, cascading, rolling, slumping, and slipping – have been identified [2]. Saeman [3] developed a model to compute the mean residence time based on material properties and kiln geometry, and analytical solutions that agree well with the model have since been developed [8, 9]. A predictive model for transverse mixing has also been established by Sai *et al.* [12] for particles in rolling mode. The model assumes that two layers, the passive and active layers, exist within the particle bed. The passive layer rotates with the kiln wall, and then rolls down the surface of the particle bed in a thin active layer [13]. The time required for the particles to roll down the active layer is very small compared to the time spent in the passive layer, but the bed depth and axial residence time of the material is calculated using the kiln geometry and angle of repose of the material. Studies using such models have generally shown feed rate has little impact

on the mean residence time; however, the mean residence time scales with particle aspect ratio and is inversely related to rotary speed and kiln incline [3, 14, 15, 16, 17, 18].

While recognizing such trends aid in kiln operation, the mean residence time alone fails to provide insight into the axial dispersion of the particles and therefore the overall quality of the treated feed. For this, the residence time distribution, a probability distribution characterizing the flow profile of a material, must be measured [19, 20]. The width of the distribution depends on material flow determined by material properties and operating conditions. Narrower distributions are indicative of yielding a more uniform product. Experimentally, this can be measured by injecting tracer particles and observing them at the outlet [21]. This has been done for millimeter-sized particles including extrudates, sand and broken rice grains [3, 14, 15]. For extrudates, Gao *et al.* [3] found that the axial dispersion coefficient of millimeter-sized extrudates decreased with rotary speed and incline angle. Higher feed rates and larger angle of repose of the materials led to higher fill levels, reducing axial dispersion. Similar trends were seen in sand and rice grains by Njeng *et al.* in a pilot plant kiln equipped with square and rectangular lifters [14, 15].

In the aforementioned work, the cohesion of the feed material was considered negligible [3, 14, 15]. The goal of this research is therefore to extend the material database gained form previous kiln studies through study of a dry cohesive powder. While powders are widespread in industry, predicting and characterizing their flow is difficult due to several factors. In rotary kilns, product uniformity depends on kiln geometry and operating conditions [27, 28, 29]. Particles also segregated depending on their density, aspect ratio, and the intensity of the cohesion [27, 28, 29, 30]. Cohesion in particular has been marked for its major effect on the mixing process and therefore the uniformity of products [22]. In recent simulations and

experiments, it was found that low degree of cohesion increased mixing, while high cohesion slowed mixing [8, 35]. Debacq *et al.* [36, 37] has also provided a hydrodynamic model for the transverse motion of cohesive powders in flighted rotary kilns. Still, residence time and axial dispersion coefficient trends for the material were absent from literature. In our experiments, tracer studies following a methodology by Danckwerts [22] were conducted at room temperature using a dry cohesive powder as feedstock seeking similar trends to those found for extrudates.

Chapter 2

Methods

Measurement of Mean Residence Time

The mean residence time was calculated from the mass holdup, measured at the end of each experiment by shutting off the feed and collecting the powder remaining in the kiln.

$$\tau_{holdup} = \frac{M}{\dot{m}} \tag{1}$$

where τ_{holdup} is the mean residence time, M is the mass hold up, and $\dot{m}$ is the mass flow rate of the material. The measured τ_{holdup} was then used to validate the prediction of mean residence time proposed by Sullivan (Equation 6).

$$\tau_{Sullivan} = \frac{1.77(\theta)^{0.5} Lf}{\varphi DN} \tag{2}$$

where θ the angle of repose of the material, L is the length of the kiln, φ is the incline of the kiln, D is the diameter of the kiln, and N is the rotary speed. A coefficient for flow f is included to account for obstructions in flow due to modifications such as lifters. A value of f = 1 was initially assumed to determine the accuracy of the model during each experiment, defining f as the ratio of τ_{holdup} to $\tau_{Sullivan}$.

$$f = \frac{\tau_{Holdup}}{\tau_{Sullivan}} \tag{3}$$

Residence Time Distribution and Axial Dispersion Coefficient

The residence time distribution was calculated using the following equation [19]:

$$E(t) = \frac{C(t)}{\int C(t)dt} \tag{4}$$

where *E(t)* is the residence time distribution and *C(t)* is the concentration of tracer particles at time *t*.

The axial dispersion model was used to represent the residence time distribution under the following assumptions [14, 40, 41]:

(i) the conditions reached steady state;

(ii) a delta-dirac tracer pulse was a function only of time and axial position;

(iii) the axial convective velocity and axial dispersion coefficient of tracer particles was constant for stable operating conditions.

The model considers axial motion of the particles as two components: a convective compontent arising from the bulk motion of the material and a diffusive component arising from the random motion of the particles. This can be represented by the Fokker-Planck equation, which describes the evolution of particle distribution in continuous systems [11, 37].

$$\frac{\partial C}{\partial t} = \frac{1}{Pe}\frac{\partial^2 C}{\partial x^2} - \frac{\partial C}{\partial x} \tag{5}$$

where

$$Pe = \frac{l}{V_x D_{ax}} \tag{6}$$

where *Pe* is the Peclet number, *l* is the length traveled by the tracer, *D* is the axial dispersion coefficient, and v_x is the axial velocity of the particles. Several analytical solutions have been

presented for granular materials [38, 39, 40]., but the Taylor [36, 37, 38] dispersion solution was used (Equation 4).

$$E(\varepsilon,\theta) = \frac{Pe^{0.5}}{(4\pi\theta)^{0.5}} e^{-\frac{Pe(\varepsilon-\theta)^2}{4\theta}} \quad (7)$$

where $\theta = \frac{t}{\tau_{Taylor}}$ and $\varepsilon = \frac{x}{l}$ represent the dimensonless time and location of the material in the kiln, respectively; and τ_{Taylor} is the mean residence time, implicitly calculated from the experimental data.

Experimental Setup

Experiments were conducted in two pilot plant rotary kilns at atmospheric temperature and pressure. In each kiln, a pulse test method developed by Danckwerts [21] was used to determine the residence time distribution. Undyed powder was fed into the kiln at a constant feed rate. At steady state, the kiln was turned off for approximately one minute to inject tracer particles into the kiln using a spoon 2.5 inches long, 2 inches wide and 1.5 inches deep. A pulse injection was assumed, so the spoon dimensions were neglected in analysis of the data. Mixtures of tracer and undyed powder exit the kiln at the outlet at 30 second intervals until tracer was invisible to the eye. As tracer was distinguishable from the undyed powder by its black color, the concentration *C(t)* was determined as a function of time based on the % reflectance of each sample at a given time *t*. Operating conditions were chosen based on previous experiments [3] and equipment capabilities.

Setup 1: Rotary Kiln with Triangular Lifters

The kiln had an internal diameter of 4 inches and a length of 90 inches, giving an L/D ratio of 22.5. Three sets of lifters spanned 70% of the kiln length, starting from the inlet. Each set

contained four lifters, five inches apart from each other set equiangular from each other along the circumference of the kiln. Each lifter had a base of 2.5 inches, a height of 0.25 inches and a length of 8.5 inches (Figure 2).

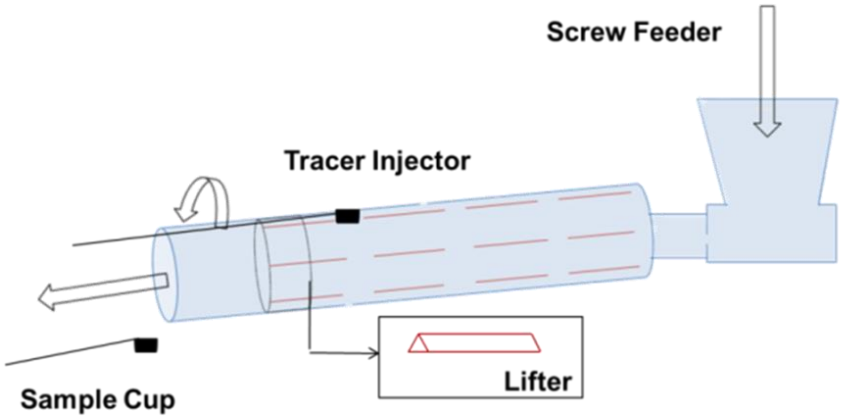

Figure 2. Rotary Kiln Equipped with Triangular Lifters

The matrix of experiments conducted is summarized below in Table 1. A screw feeder fed material into the kiln at constant rates of 1 lb/hr or 5 lb/hr. A control panel set kiln speeds to 3.5, 4.0 or 4.5 RPM. A jack mechanism at the inlet of the kiln adjusted the incline angle to 2.0º or 4.0º. A fixed circular dam at the inlet prevented backward leakage of materials; the maximum operation fill level without backward leakage was about 15%. Operating fill levels during experiments ranged from 2% to 10%.

Table 1. Matrix of Operating Conditions for Setup 1

Operation Variables	**Conditions**
Incline angle φ (°)	2.0, 4.0
Rotary speed (rpm)	3.5, 4.0, 4.5
Feed Rate (lb/hr)	1.0, 5.0

Setup 2: Rotary Kiln with a Circular Lifter

The kiln had an internal diameter of 6 inches and a length of 120 inches, giving an L/D ratio of 20. A single circular lifter with a diameter of 5 5/8 inches spanned the length of the kiln. (Figure 3).

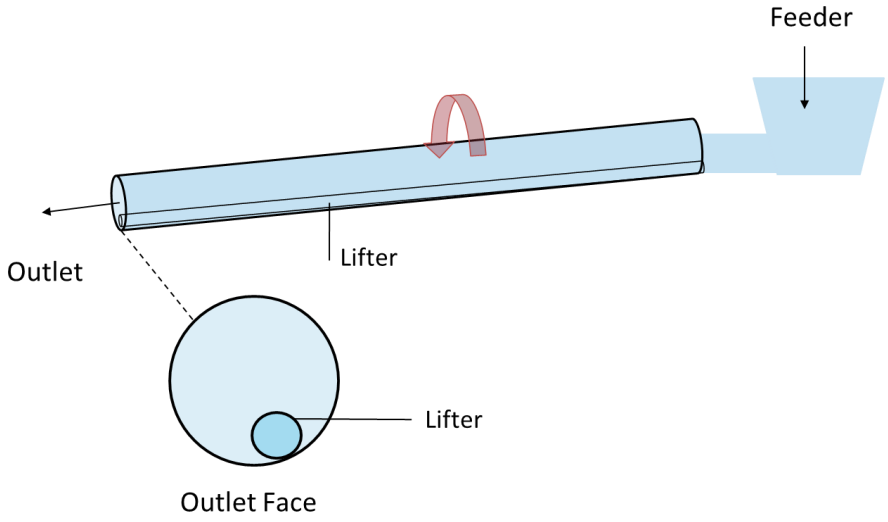

Figure 3. Rotary Kiln with a Singular Circular Lifter

The experiments conducted in this setup were designed to extend those conducted in the first setup. Again, operating fill levels during experiments ranged from 2% to 10%, corresponding to a minimum feed rate of 1 lb/hr and a maximum of 12 lb/hr. A control panel set kiln speeds to 2.0, 3.5, 4.0 or 4.5, 8.0 and 16.0 RPM. A jack mechanism at the inlet of the kiln adjusted the incline to angles between 2.0º and 5.0º. The full set of conditions can be found below in Table 3.

Table 2. Matrix of Operating Conditions for Setup 2

Operation Variables	Conditions
Incline angle φ (°)	2.0, 3.0, 4.0, 5.0
Rotary speed (rpm)	2.0, 3.5, 4.0, 4.5, 8.0, 16.0
Volumetric feed rate (lb/hr)	1.5, 3.0, 6.0, 12.0

Materials

In each kiln, a different industrial fluid catalytic cracking (FCC) powder was used as the feed. The powders were chosen because of their industrial relevance and to further extend the library of materials used in previous work. Measured material properties can be found below in Table 3. The loose bulk density was measured using the mass of material required to fill a 100 mL graduated cylinder. The static angle of repose was measured using a fixed funnel method.

Table 3. Measured Material Properties of Feed

Experimental Setup	Material	Diameter (mm)	Bulk density (g/cm^3)	Static angle of repose (º)
Setup 1	FCC Catalyst (W.R. Grace)	0.08	0.76	37.0
Setup 2	FCC Catalyst (BASF)	0.07	0.79	32.0

An incipient wetness impregnation using cobalt (II) nitrate hexahydrate was performed for each material to create the tracer. The powder contained 10 wt% cobalt oxide following calcination at

538ºC for 8 hours. The measured loose bulk density and the static angle of repose of the material were unchanged by the dying process.

Sample Analysis

The concentration of tracer particles was measured using a spectrophotometer according to a methodology developed by Emady *et al* [42]. This offline detection digital imaging analysis method was selected since previous studies have shown that inline solid sampling can be invasive and slow, disrupting particle movement [43]. The spectrophotometer was used to analyze each mixture by measuring the % reflectance corresponding to each concentration (Figure 4). The data shown was taken at an incline of 2°, 3.5 rpm and a feed rate of 1 lb/hr.

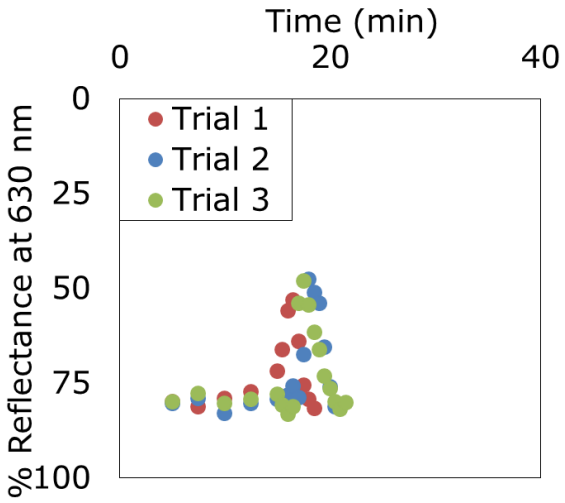

Figure 4. % Reflectance vs. Time.

To obtain *C(t)* and therefore calculate *E(t)*, a calibration curve was developed using % reflectance data from of mixtures of 0%, 5%, 10%, 15%, 20%, and 25% undyed to dyed powder (Figure 5). The resulting concentration curve was then used to obtain the residence time distribution (Equation 4).

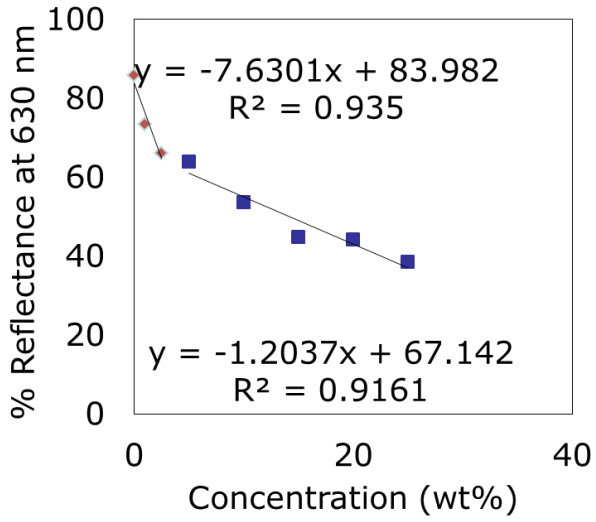

Figure 5. Example of Spectrophotometer Calibration Curve.

Chapter 3

Results and Discussion

Mean Residence Time

Setup 1: Rotary Kiln with Triangular Lifters

Figure 6 shows the comparison among the experimental data, the Taylor fit and Sullivan's model at both 2° and 4° (Figure 6). Generally, both the Taylor fit and Sullivan's model underestimated the experimental mean residence time τ_{holdup}. This occurred due to the presence of the lifters, which increased the mean residence time by causing back mixing of the particles as they traveled along the particle bed. The same results were found by Njeng *et al.* [14, 15]. An increase in incline was found to decrease the mean residence time, as predicted by Sullivan; however, feed rate unexpectedly effected the mean residence time while the rotary speed had little effect. The rotary speed may have had little effect due to the irregularity of the

particle flow behavior within the kiln; the velocity profile may was discontinuous due to the large fraction of the power bed consumed by the lifters, hindering the effect of rotary speed.

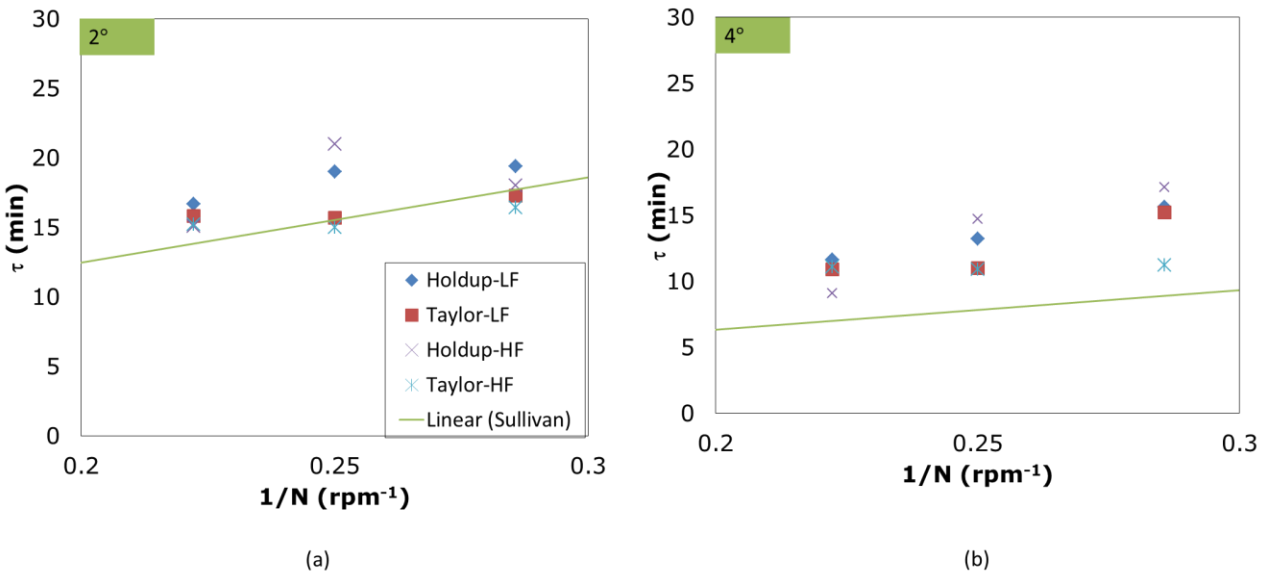

Figure 6. Mean Residence Time Data for Setup 1 at (a) 2° and (b) 4°

The deviations of the experimental data from Sullivan's model were quantified by calculating the coefficient for flow *f* at each operating condition using Equation 7. Generally, the Sullivan model underestimated τ_{holdup}, with $f \geq 1.0$ (Table 4). This inaccuracy generally increased with in incline; τ_{Holdup} was nearly double that of $\tau_{Sullivan}$ at a feed rate of 1 lb/hr at 4°, with an exception of the transition between 4.0 rpm and 4.5 rpm at a feed rate of 5 lb/hr at 4°. Sullivan's model was found to be more accurate at this rotary speed. In this case, the velocity of the particles may have been so charged that the particle bed approached plug-flow like behavior, and Sullivan's model became more accurate. This effect as more pronounced at 2°; at this incline, the contribution of the axial velocity by the feed rate may have dominated that of rotation, whose primary function is to improve mixing.

The Taylor dispersion fit reasonably matched these data, falling between τ_{holdup} and $\tau_{Sullivan}$ at each operating condition. The accuracy of the fit increased with feed rate. Inaccuracies may again have been introduced by the lifters; each group of lifters was set at a distance of 5 inches apart, allowing the lifters to intermittently influence bed mixing. It was possible that the lifter geometry segregated the tracer pulse particles from one another, skewing results.

Table 4. Flow Coefficient f for Setup 1

		Incline (°)	
		2	**4**
Feed Rate (lb/hr)	**Rotary Speed (rpm)**	**f**	
1	3.5	1.1	1.8
	4	1.2	1.7
	4.5	1.2	1.7
5	3.5	1.0	1.9
	4	1.3	1.9
	4.5	1.1	1.3

Setup 2: Rotary Kiln with a Circular Lifter

In Figure 7, τ_{holdup}at both low feed (LF) and high feed (HF) are compared to τ_{Taylor} and $\tau_{Sullivan}$ at both 2° and 4°. At 2°, τ_{Taylor} and $\tau_{Sullivan}$ reasonably matched τ_{holdup}. Inaccuracies and variations in measurements were more prevalent at an incline of 4°. This is may be due more unpredictable behavior of the particles at a higher velocity due to the incline of the kiln; holdup data at an incline of 4° also did not follow the linear trend observed in hold up data taken during experiments conducted at 2°.

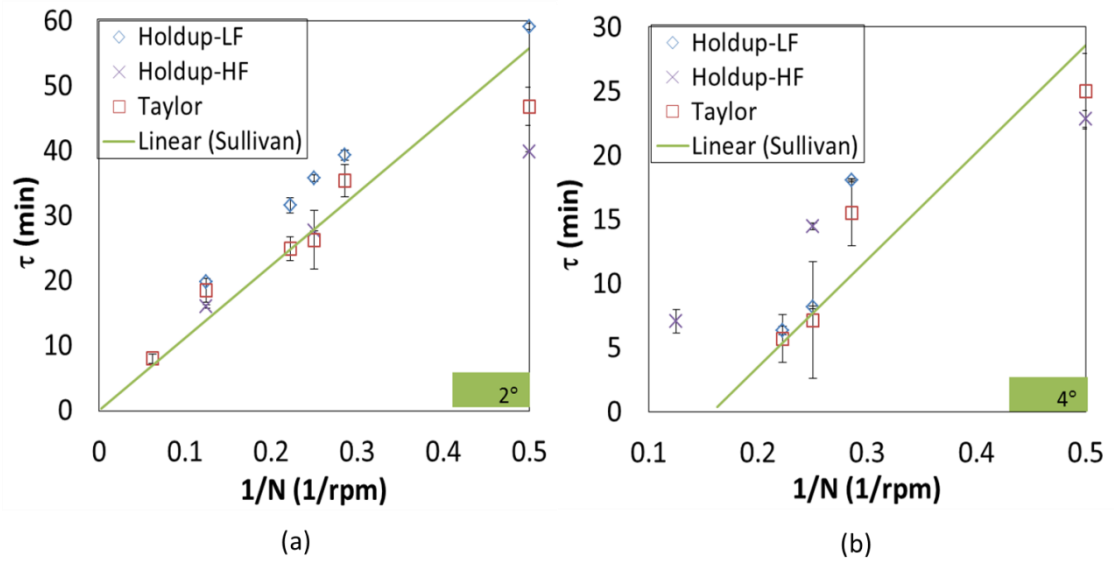

Figure 7. Mean residence time versus the inverse of rotary speed. At (a) 2° and (b) 4°

It was found that at low feed rate, Sullivan's model underestimated time, with $f > 1.0$. The underestimation increased with an increase in incline and in rotary speed. At high feed rate, however, Sullivan's model overestimated the actual mean residence time, with $f < 1.0$ at low rotary speeds. At 4.0 rpm and 8.0 rpm, $f = 1$, signifying that Sullivan's model accurately predicted the actual mean residence time. The accuracy of Sullivan's model therefore improved with an increase in feed rate. The dependency of f on rotary speed also decreased at both inclines at the high feed rate.

Table 5. Coefficient of Flow f for Setup 2

	Feed Rate (lb/hr)	3		12	
		f			
	Incline (°)	2.0	4.0	2.0	4.0
N (rpm)	2.0	1.1	1.2	0.7	0.8
	3.5	1.2	N/A	N/A	N/A
	4.0	1.3	1.3	1.0	1.0
	4.5	1.3	N/A	N/A	N/A
	8.0	1.4	1.2	1.1	1.0
	16.0	1.5	1.8	1.2	1.1

When intermediate feed rates were tested at the same incline and rotary speed (2° and 4 rpm), however, *f* increased from a feed rate of 1.5 lb/hr to 6.0 lb/hr. At a feed rate of 12 lb/hr, the axial velocity of the particles charged by the feed rate dominated the effects of the other operating conditions, allowing the material to move quickly enough to neglect the other operating conditions. The material bed moved more like a plug, moving axially more quickly than it mixed, allowing for Sullivan's model to match the experimental mean residence time.

While these results corresponded to a higher feed rate than used in Setup 1, each feed rate actually corresponded to the same fill level of 10%. This indicated that at a minimum fill level of

10%, Sullivan's model was applicable, despite differences in kiln geometry and material properties.

Table 6. Coefficient of Flow f at Different Feed Rates

Feed Rate (lb/hr)	f
1.5	1.2
3.0	1.3
6.0	1.4
12.5	1.0

Residence Time Distribution and Axial Dispersion Coefficient

The residence time distribution E(t) was obtained for each trial conducted at each operating condition. While variation was seen among the trials, the Taylor dispersion fit adequately modeled the data (Figure 8). In succeeding figures, the E(t) curves displayed are therefore average curves. The value of C(t) at each time point was averaged across the three trials to obtain an average E(t).

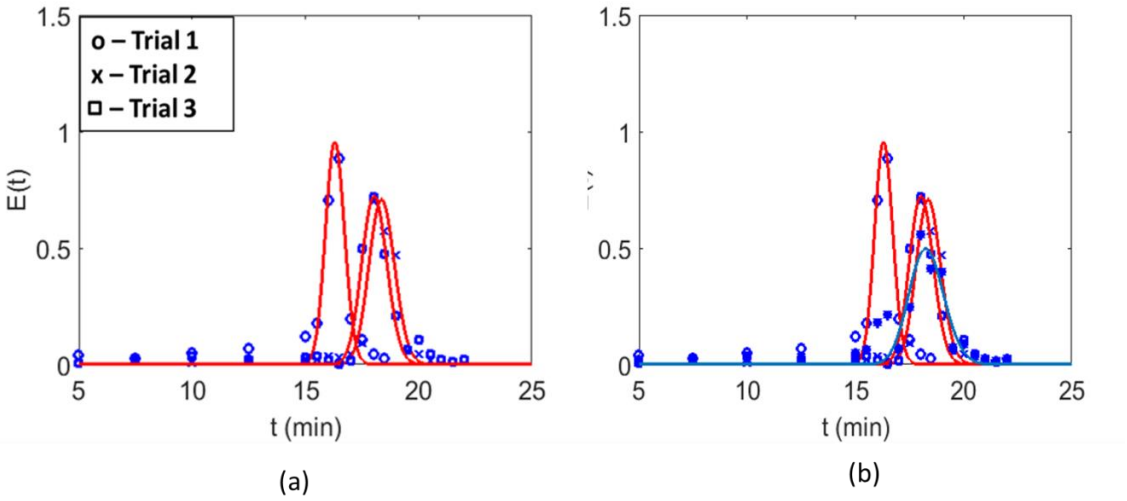

Figure 8. Residence Time Distribution Data.

Effect of Rotary Speed and Mean Residence Time

Overall, an increase in rotary speed narrowed the residence time distribution and decreased the mean residence time, as shown in Figure 9. Limitations to this effect were seen between 8.0 rpm and 16.0 rpm. From 8.0 rpm to 16.0 rpm, the residence time distribution narrowed, but the curves overlapped, indicating close values in mean residence time despite doubling of rotary speed from 8.0 rpm to 16.0 rpm. This overlap was in agreement with Sullivan's prediction of the mean residence time, but in disagreement with the experimental residence time; according to the holdup data, the mean residence time was 20 minutes at 8.0 rpm and 11 minutes at 16.0 rpm (Figure 7). This therefore exposed a limitation of the Taylor dispersion fit and Sullivan's model.

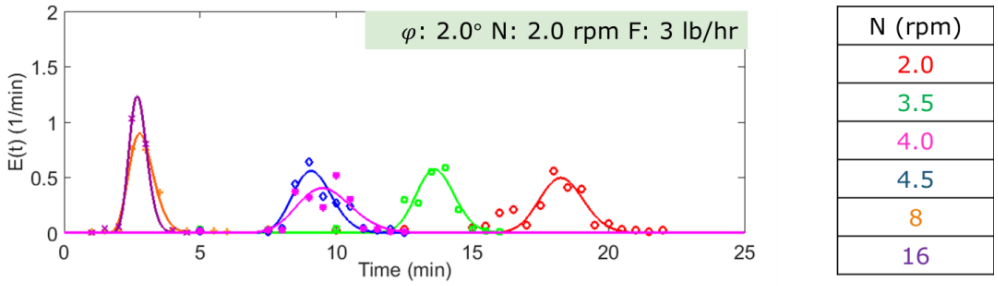

Figure 9. Residence Time Distribution at Increasing Rotary Speeds.

The value of the axial dispersion coefficient was less sensitive to changes in rotary speed than the residence time distribution was. From 4.0 rpm to 8.0 rpm, the values of D_{ax} were similar, with a standard deviation of 0.1. At 16.0 rpm, however, an increase by roughly ten times the value of D_{ax} at 4.0 rpm was observed (Figure 10). It was expected that a narrow residence time distribution would produce a low value of D_{ax}. At 16 rpm, however, the particle bed appeared to exit the rolling regime and flowed more erratically, producing dust as it flowed along the kiln. This indicated that various regimes of particle flow occurred across the experiments.

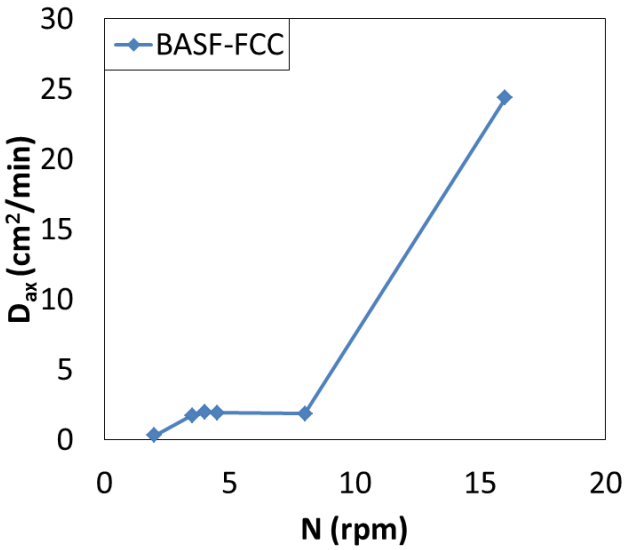

Figure 10. Axial Dispersion Coefficient D_{ax} versus Rotary Speed N. Data is shown here for an incline of 2° and a feed rate of 3 lb/hr.

Effect of Kiln Incline

Increasing the kiln incline from 2° to 4° decreased the mean residence time. The shape of the residence time distribution, however, became less predictable. Overall, an increase in incline narrowed the residence time distribution (Figure 11). As rotary speed increased, however, the narrowness of the residence time distribution fluctuated.

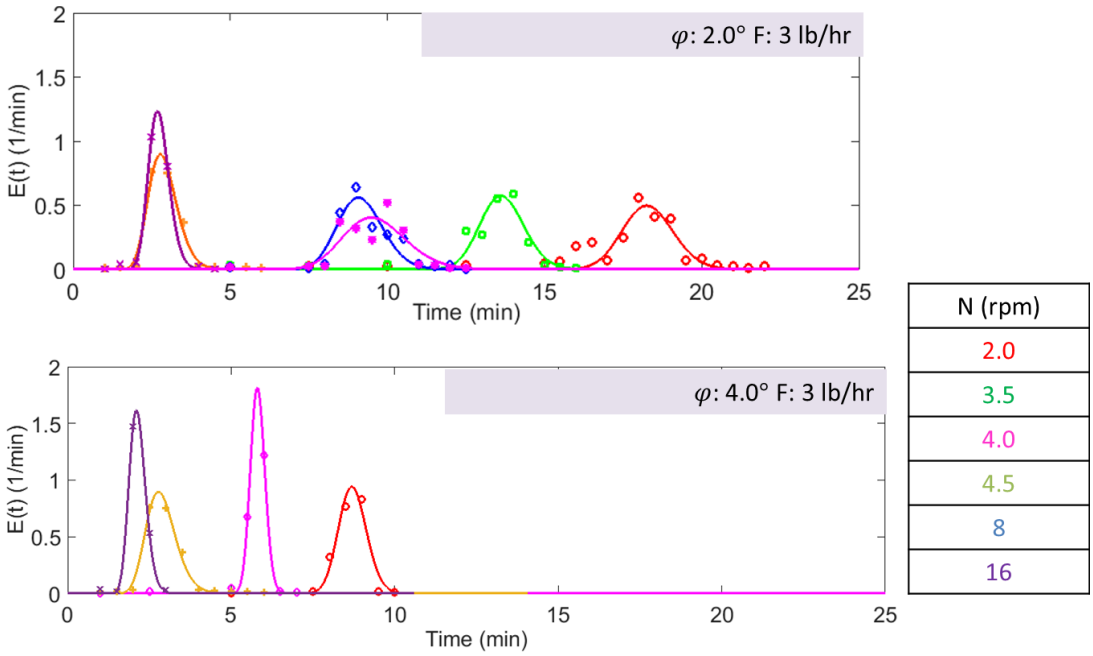

Figure 11. Residence Time Distributions at Increasing Incline.

Such trends were not seen in the axial dispersion coefficient, which showed a direct relationship to rotary speed (Figure 12). This reiterated the findings found at low incline – that is, a narrow residence time distribution is not an indicator of a low value of the axial dispersion coefficient. Axial dispersion was relatively small, but the value of the coefficient was large.

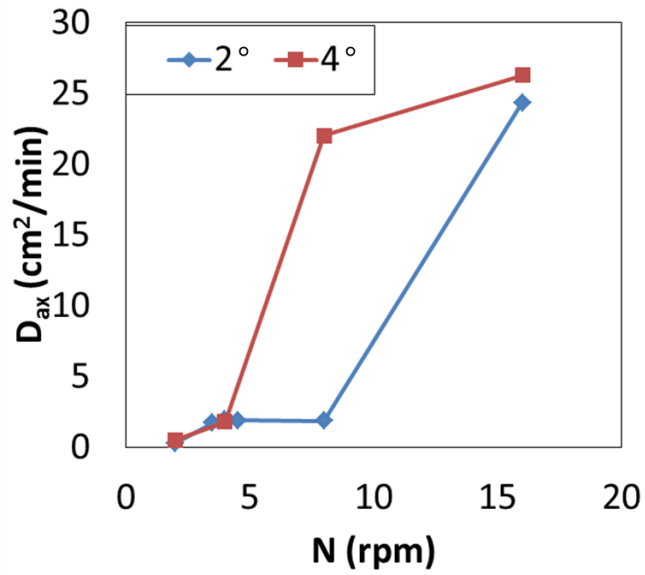

Figure 12. Axial Dispersion Coefficient vs. Rotary Speed at 2° and 4°

No effect by incline was seen on the axial dispersion coefficient at rotary speeds of 2.0 rpm and 4.0 rpm. At 8.0 rpm, however, the axial dispersion coefficient was 22.0 cm^2/min, almost equal to the value at 16.0 rpm at 2°. At the high incline, particle flow behavior changed at a lower rotary speed than at low incline. The values at 16.0 rpm approach one another, perhaps indicating a limit to the axial dispersion coefficient.

Effect of Feed Rate

The residence time distribution data supported the fact the mean residence time lost its dependency on feed rate 12 lb/hr, as indicated by the values of the flow coefficient *f*. From 1.5 lb/hr to 6 lb/hr, the residence time distribution shifted to shorter times and narrowed. The mean residence time decreased. At 12 lb/hr, however, the residence time distribution appeared in the middle of the residence time distributions found at lower feed rates. The mean residence time decreased from 6 lb/hr to 12 lb/hr, though the residence time distribution again narrowed.

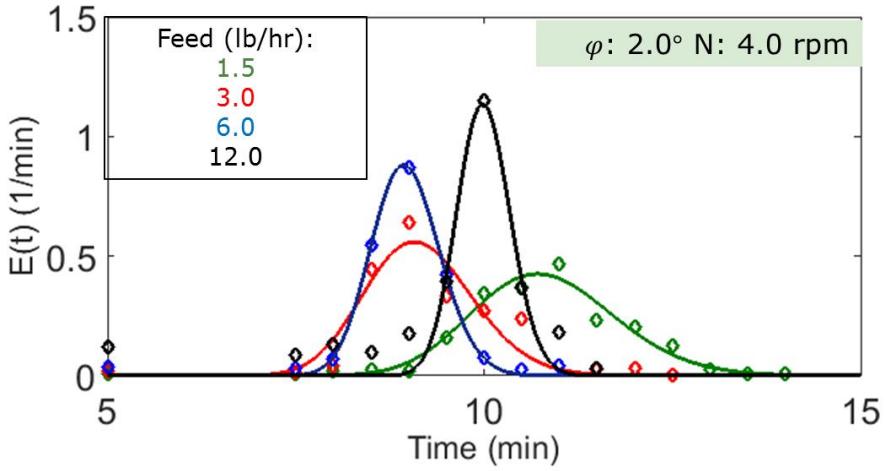

Figure 13. Residence Time Distributions at Increasing Feed Rate

In this case, a narrowing of the residence time distribution indicated a smaller axial dispersion coefficient (Figure 14). As values of *f* decreased with feed, this corresponded to a more "plug like" flow of the feed, and therefore a lower value of the axial dispersion coefficient.

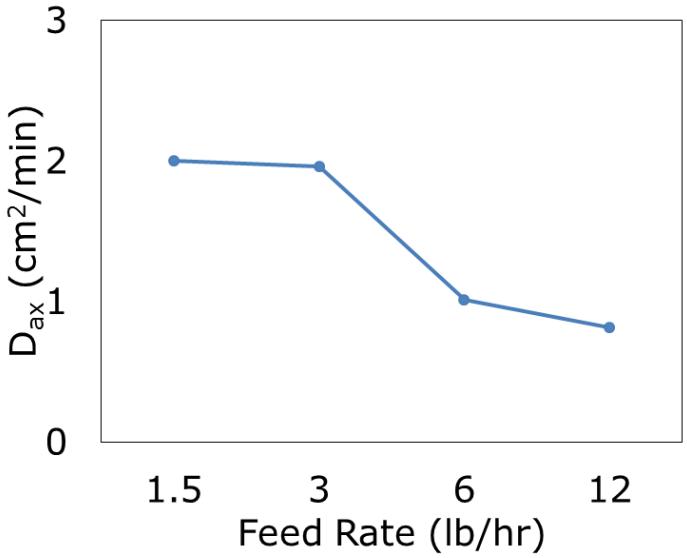

Figure 14. Axial Dispersion Coefficient D_{ax} vs. Feed Rate

Overall, these trends collapse to an inverse relationship of the axial dispersion coefficient to the mean residence time (Figure 15). Given a set operating parameters, then, the dispersion can be determined.

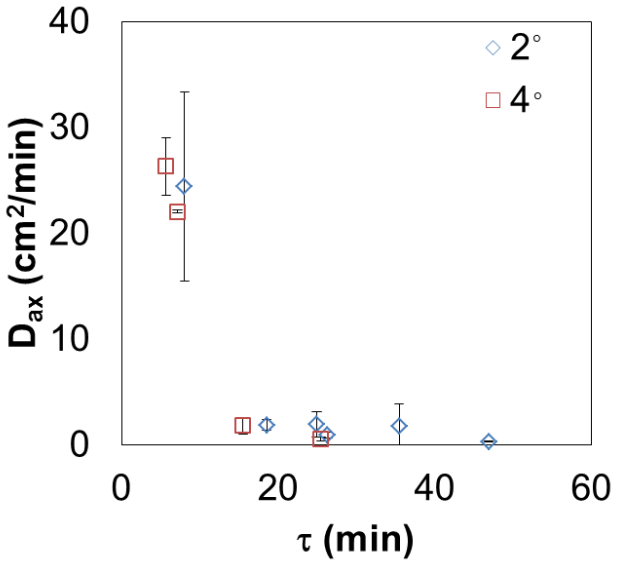

Figure 15. Axial Dispersion Coefficient D_{ax} versus Mean Residence Time τ at 2° and 4°

Comparison to Other Measurements of D_{ax}

The axial dispersion coefficients from both setups were compared those of extrudates found by Gao *et al.* [3] as well as to a measurement conducted in a small batch experiment conducted by Koynov *et al.* relating D_{ax} to bulk flow properties [45] (Figure 16). In both setups, the axial dispersion coefficient was found to exceed the measurement made by Koynov. In her study, D_{ax} was calculated using Fick's second law and therefore neglected the impact of incline on bulk flow. Our results therefore showed that the influence of incline was therefore significant at high enough rotary speeds. Still, the measured axial dispersion coefficients for each catalyst were found to be very similar despite differences in kiln length, diameter and lifter orientation. The axial dispersion coefficient was therefore found predictable based solely on the axial velocity determined by the material feed rate and rotary speed. A limitation may exist due to material properties, as the measurements for extrudates produced a similar trend to the cohesive powders, just at increased values of the axial dispersion coefficient.

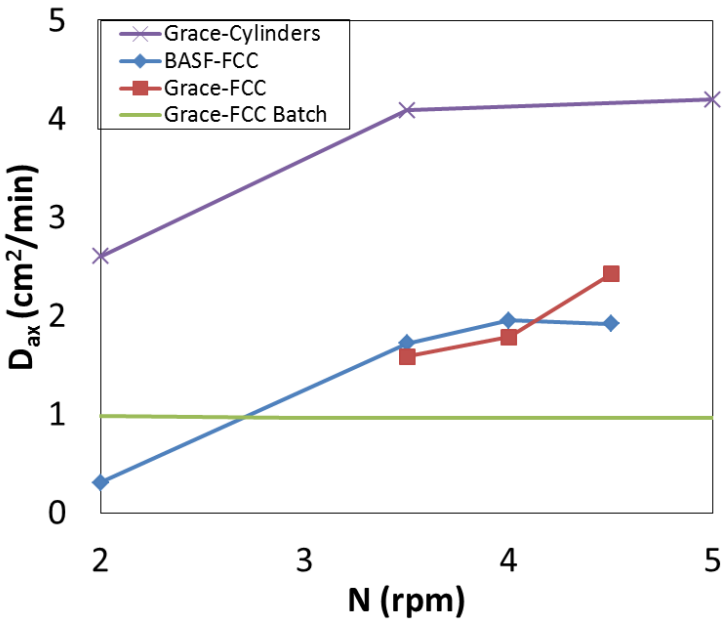

Figure 16. Comparison of Axial Dispersion Coefficients D_{ax}

Conclusions and Future Work

In this work, the axial dispersion coefficient was determined for dry cohesive powders using the Taylor dispersion fit to the axial dispersion model. Previously used to determine the axial dispersion coefficient for free-flowing materials like extrudates, the model was used successfully for dry cohesive powders for the first time. The axial dispersion coefficient was found to be greater than a batch measurement done using Fick's second law, which neglected the effect of bulk flow. The effect of continuous flow and incline was therefore significant in determining the axial dispersion coefficient. Overall, the axial dispersion coefficient increased with a decrease in residence time. Comparing the two systems studied, it was found that the geometry of the kiln – its length, diameter, and lifter orientation – had an insignificant effect on the axial dispersion coefficient.

Overall, kiln geometry only effected the residence time. Generally, the experimental residence time exceeded the time predicted by the Sullivan model and the Taylor dispersion fit. This was attributed to the presence of lifters, which increased the residence time of the particles by encouraging back mixing. Still, both fits provided a reasonable estimate of the measured mean residence time. Limitations of the Taylor fit were seen at high rotary speeds and high incline. The Sullivan model was found to be more accurate at high feed and low incline angles. Future work must be done to improve the accuracy of the model to better account for the effects of feed rate and geometry. The effect of heating and calcination on particle flow should also be studied.

Appendix A

Standard Operating Procedure for Calciner Tracer Study

Preparation

1. Prior to the start of the experiment, record the time, temperature and humidity data available for the location.
2. Set the calciner incline, rotary speed and feed rate to desired levels.
3. Load the feeder with powder.
4. Allow the calciner to run until the outlet feed rate is constant. This typically takes 1 – 1.5 times the mean residence time of the particles. Sullivan's model can be used to get a somewhat accurate prediction.
    a. Measure the feed rate every five minutes by collecting and weighing mass samples until they are constant.
    b. Check where the feeder drops off the material. If it is not directly at the start of the calciner tube, measure the distance between the inlet face and the drop off point. Calculate the holdup of this region to determine if it is significant enough to effect results.
5. Once the flow is steady, take a 1-minute video from the calciner outlet to get a view of particle behavior at that operating condition.

Tracer Study

1. Mass and collect the desired amount of tracer required for the study.
2. Shut off the calciner completely, so that is no longer receiving material from the inlet or rotating.
3. Introduce the tracer at a distance 45'' from the calciner outlet using a spoon.
4. Turn the calciner back on, allowing tracer to mix and flow with the particle bed.
5. Collect samples every 5 minutes for 30 seconds at a time from the time the calciner is turned back on.
6. When tracer is visible in the sampling cup, continuously collect samples for 30 seconds at a time until tracer is no longer visible.
7. Following the tracer study, empty the calciner and mass the holdup.

* For 2 and 4, it may be helpful to have someone else shut down and turn on the calciner to reduce the amount of lag time

References

1. Brook, R.; Cahn, R.; Bever, M. *Concise Encyclopedia Of Advanced Ceramic Materials*; Pergamon Press: Oxford, 1991.
2. Akwasi A. Boateng, 1 - The Rotary Kiln Evolution and Phenomenon, In Rotary Kilns, edited by Akwasi A. Boateng, Butterworth-Heinemann, Burlington, 2008, Pages 1-14, ISBN 9780750678773, http://dx.doi.org/10.1016/B978-075067877-3.50003-9. (http://www.sciencedirect.com/science/article/pii/B9780750678773500039)
3. Saeman WC. Passage of solids through rotary kilns: factors affecting time of passage. Chem Eng Prog. 1951;47:508–514.
4. Gao, Y., Glasser, B. J., Ierapetritou, M. G., Cuitino, A., Muzzio, F. J., Beeckman, J. W., Fassbender, N. A. and Borghard, W. G. (2013), Measurement of residence time distribution in a rotary calciner. AIChE J., 59: 4068–4076. doi: 10.1002/aic.14175
5. Boateng AA, Barr PV. A thermal model for the rotary kiln including heat transfer within the bed. Int J Heat Mass Transfer. 1996;39(10): 2131–2147.
6. Li SQ, Ma LB, Wan W, Yao Q. A Mathematical Model of Heat Transfer in a Rotary Kiln Thermo-Reactor. Chem Eng Technol. 2005;28(12):1480–1489.
7. Chaudhuri B, Muzzio FJ, Tomassone MS. Modeling of heat transfer in granular flow in rotating vessels. Chem Eng Sci. 2006;61(19):6348–6360.
8. Thammavong P, Debacq M, Vitu S, Dupoizat M. Experimental apparatus for studying heat transfer in externally heated rotary kilns. Chem Eng Technol. 2011;34(5):707–717.
9. Liu XY, Zhang J, Specht E, Shi YC, Herz F. Analytical solution for the axial solid transport in rotary kilns. Chem Eng Sci. 2009;64(2):428–431.
10. Liu XY, Specht E. Mean residence time and hold-up of solids in rotary kilns. Chem Eng Sci. 2006;61(15):5176–5181.
11. Henein H, Brimacombe J, Watkinson A. The modeling of transverse solids motion in rotary kilns. Metall Mater Trans B. 1983;14(2):207–220.
12. Sherritt RG, Chaouki J, Mehrotra AK, Behie LA. Axial dispersion in the three-dimensional mixing of particles in a rotating drum reactor. Chem Eng Sci. 2003;58(2):401–415.

13. Sai P, Surender G, Damodaran A, Suresh V, Philip Z, Sankaran K. Residence time distribution and material flow studies in a rotary kiln. Metall Mater Trans B. 1990;21(6):1005–1011.
14. Sherritt, R.G., Caple, R., Behie, L.A., Mehrotra, A.K., 1994. The movement of solids through flighted rotating drums. 2. Solids gas interactions and model validation. Canadian Journal of Chemical Engineering 72 (2), 240–248.
15. O.S. Sudah, D. Coffin-Beach, F.J. Muzzio, Effects of blender rotational speed and discharge on the homogeneity of cohesive and free flowing mixtures, Int. J. Pharm. 247 (2002) 57–68.
16. A.S. Bongo Njeng, S. Vitu, M. Clausse, J.-L. Dirion, M. Debacq, Effect of lifter shape and operating parameters on the flow of materials in a pilot rotary kiln: Part I. Experimental RTD and axial dispersion study, Powder Technology, Volume 269, January 2015, Pages 554-565, ISSN 0032-5910, http://dx.doi.org/10.1016/j.powtec.2014.03.066. (http://www.sciencedirect.com/science/article/pii/S0032591014002885)
17. A.S. Bongo Njeng, S. Vitu, M. Clausse, J.-L. Dirion, M. Debacq, Effect of lifter shape and operating parameters on the flow of materials in a pilot rotary kiln: Part II. Experimental hold-up and mean residence time modeling, Powder Technology, Volume 269, January 2015, Pages 566-576, ISSN 0032-5910, http://dx.doi.org/10.1016/j.powtec.2014.05.070. (http://www.sciencedirect.com/science/article/pii/S0032591014005452)
18. M.E. Sheehan, P.F. Britton, P.A. Schneider, A model for solids transport in flighted rotary dryers based on physical considerations, Chemical Engineering Science, Volume 60, Issue 15, August 2005, Pages 4171-4182, ISSN 0009-2509, http://dx.doi.org/10.1016/j.ces.2005.02.055. (http://www.sciencedirect.com/science/article/pii/S0009250905001788)
19. Sherritt, R.G., Caple, R., Behie, L.A., Mehrotra, A.K., 1993. The movement of solids through flighted rotating drums. Part 1: Model formulation. The Canadian Journal of Chemical Engineering 71, 337–346.
20. Yijie Gao, Fernando J. Muzzio, Marianthi G. Ierapetritou, A review of the Residence Time Distribution (RTD) applications in solid unit operations, Powder Technology, Volume 228, September 2012, Pages 416-423, ISSN 0032-5910,

http://dx.doi.org/10.1016/j.powtec.2012.05.060.
(http://www.sciencedirect.com/science/article/pii/S0032591012003889)

21. Gao Y, Vanarase A, Muzzio F, Ierapetritou M. Characterizing continuous powder mixing using residence time distribution. Chem Eng Sci. 2011;66(3):417–425.
22. Danckwerts PV. Continuous flow systems: distribution of residence times. Chem Eng Sci. 1953;2(1):1–13.
23. K. Rietema, "Powders, what are they?," *Powder Technology,* vol. 37, pp. 5-23, 1984.
24. A. Alexander, *et al.*, "Scaling surface velocities in rotating cylinders as a function of vessel radius, rotation rate, and particle size," *Powder Technology,* vol. 126, pp. 174-190, 2002.
25. S. J. Rao, *et al.*, "Axial transport of granular solids in rotating cylinders. Part 2: Experiments in a non-flow system," *Powder Technology,* vol. 67, pp. 153-162, 1991.
26. D. K. Singh, *A Fundamental Study of the Mixing of Solid Particles*: University of Rochester, 1979.
27. A.-Z. Abouzeid, T. Mika, K. Sastry, D. Fuerstenau, The influence of operating variables on the residence time distribution for material transport in a continuous rotary drum, Powder Technol. 10 (6) (1974) 273–288.
28. T. Shinbrot, A. Alexander, F.J. Muzzio, Spontaneous chaotic granular mixing, Lett. Nat. 397 (1999) 675–678.
29. O.S. Sudah, D. Coffin-Beach, F.J. Muzzio, Quantitative characterization of mixing of free-flowing granular material in tote (bin)-blenders, Powder Technol. 126 (2002) 191–200.
30. O.S. Sudah, D. Coffin-Beach, F.J. Muzzio, Effects of blender rotational speed and discharge on the homogeneity of cohesive and free flowing mixtures, Int. J. Pharm. 247 (2002) 57–68.
31. S. Das Gupta, D.V. Khakhar, S.K. Bhatia, Axial segregation of particles in a horizontal rotating cylinder, Chem. Eng. Sci. 46 (5–6) (1991) 1513–1517.
32. G.H. Ristow, Particle mass segregation in a two-dimensional rotating drum, Europhys. Lett. 28 (1994) 97.
33. K.M. Hill, J. Kakalios, Reversible axial segregation of binary mixtures of granular material, Phys. Rev., E 49 (5) (1994) R3610–R3614.

34. M.B. Donald, B. Roseman, Mixing and demixing of solid particles: Part 1. Mechanisms in a horizontal drum mixer, Br. Chem. Eng. 7 (1962) 749.
35. J.B. Knight, H.M. Jaeger, S.R. Nagel, Vibration-induced size separation in granular media: the convection connection, Phys. Rev. Lett. 70 (24) (1993) 3728–3731.
36. Bodhisattwa Chaudhuri, Amit Mehrotra, Fernando J. Muzzio, M. Silvina Tomassone, Cohesive effects in powder mixing in a tumbling blender, Powder Technology, Volume 165, Issue 2, 13 July 2006, Pages 105-114, ISSN 0032-5910, http://dx.doi.org/10.1016/j.powtec.2006.04.001.(http://www.sciencedirect.com/science/article/pii/S0032591006001070)
37. Marie Debacq, Stéphane Vitu, Denis Ablitzer, Jean-Léon Houzelot, Fabrice Patisson, Transverse motion of cohesive powders in flighted rotary kilns: experimental study of unloading at ambient and high temperatures, Powder Technology, Volume 245, September 2013, Pages 56-63, ISSN 0032-5910, http://dx.doi.org/10.1016/j.powtec.2013.04.007. (http://www.sciencedirect.com/science/article/pii/S0032591013002647)
38. Marie Debacq, Phahath Thammavong, Stéphane Vitu, Denis Ablitzer, Jean-Léon Houzelot, Fabrice Patisson, A hydrodynamic model for flighted rotary kilns used for the conversion of cohesive uranium powders, Chemical Engineering Science, Volume 104, 18 December 2013, Pages 586-595, ISSN 0009-2509, http://dx.doi.org/10.1016/j.ces.2013.09.037. (http://www.sciencedirect.com/science/article/pii/S0009250913006568)
39. Levenspiel O, Smith WK. Notes on the diffusion-type model for the longitudinal mixing of fluids in flow. Chem Eng Sci. 1957;6(4-5):227–235.
40. Risken H. The Fokker-Planck Equation: Methods of Solution and Applications, 2nd ed. New York: Springer; 1996.38. Conway SL, Liu X, Glasser BJ.
41. M.E. Sheehan, P.A. Schneider, A.Monro, S. Vigh, Transportation and Axial Dispersion of Sugar in Flighted Rotary Dryers, PK Editorial Services Pty Ltd, 2002. 469–474.
42. V. Karra, D. Fuerstenau,Material transport in a continuous rotary drum. Effect of discharge plate geometry, Powder Technol. 16 (1) (1977) 23–28.
43. Heather N. Emady, Maya Wittman, Sara Koynov, William G. Borghard, Fernando J. Muzzio, Benjamin J. Glasser, Alberto M. Cuitino, A simple color concentration

measurement technique for powders, Powder Technology, Volume 286, December 2015, Pages 392-400, ISSN 0032-5910, http://dx.doi.org/10.1016/j.powtec.2015.07.050.

44. A.U. Vanarase, F.J. Muzzio, Effect of operating conditions and design parameters in a continuous powder mixer, Powder Technology 208 (1) (2011) 26–36.
45. Sara Koynov, Yifan Wang, Agnesa Redere, Prashani Amin, Heather N. Emady, Fernando J. Muzzio, Benjamin J. Glasser, Measurement of the axial dispersion coefficient of powders in a rotating cylinder: dependence on bulk flow properties, Powder Technology, Volume 292, May 2016, Pages 298-306, ISSN 0032-5910, http://dx.doi.org/10.1016/j.powtec.2016.01.039.